DIFFERENTIAL TRACTOGRAPHY PIPELINES STUDY IN ASYMPTOMATIC INDIVIDUALS WITH CEREBRAL SMALL VESSEL DISEASE

AMANINA BINTI AHMAD SAFRI

UNIVERSITI SAINS MALAYSIA

2022

DIFFERENTIAL TRACTOGRAPHY PIPELINES STUDY IN ASYMPTOMATIC INDIVIDUALS WITH CEREBRAL SMALL VESSEL DISEASE

by

AMANINA BINTI AHMAD SAFRI

Thesis submitted in partial fulfilment of the requirements for the degree of Doctor of Neuroscience.

Feb 2022

ACKNOWLEDGEMENT

ALHAMDULILLAH

In the name of Allah, most gracious and most merciful. Praise to Almighty Allah for His endless blessings throughout this beautiful Doctorate journey. First and foremost, I would like to express my sincere gratitude to my main supervisor, Assoc. Prof. Dr Muzaimi Mustapha provided me with an opportunity to conduct this exciting research, for his continuous support of my Doctorate study and related research, and his patience, motivation, and vast knowledge. His guidance helped me in all the time of research and writing of this thesis. I could not have imagined having a better advisor and mentor for my Doctorate study. Also, I would like to thank my co-supervisors: Dr Anusha Achuthan and Dr Nur Hartini for their insightful comments and encouragements. Without their precious support, it would not be possible to conduct this research. Moreover, I would like to thank my fellow CSVD team members for their full supports and cooperation in this study: Dr Che Mohd Nasril and Puan Mazira. A very special thanks to my family. Words cannot express how grateful I am to my father; Ahmad Safri bin Dolah, my beloved mother; Zaleha Binti Mat Noor for all the sacrifices that you have made on my behalf. Your prayer for me was what sustained me thus far. Finally, I thank Allah again for letting me through all the difficulties. I could not have done this without You. I have experienced Your guidance day by day. You are the one who let me finish this wonderful journey.

Thank you, Allah.

TABLE OF CONTENTS

ACKNOWLEDGEMENT ..... **i**

TABLE OF CONTENTS ..... **ii**

LIST OF TABLES ..... **vi**

LIST OF FIGURES ..... **xi**

LIST OF ABBREVIATION ..... **xvi**

LIST OF APPENDICES ..... **xx**

ABSTRAK ..... **xxi**

ABSTRACT ..... **xxiii**

CHAPTER 1 INTRODUCTION **1**

1.1 Introduction 1

1.2 Rationale and Significance of Study 4

1.3 Objectives 5

1.3.1 General Objective 5

1.3.2 Specific Objectives 5

1.3.3 Research Question 6

1.3.4 Research Hypothesis 6

CHAPTER 2 LITERATURE REVIEW **7**

2.1 Introduction to cerebrovascular disease 7

2.1.1 Definition & Classification 7

2.1.2 Types of cerebrovascular disease 8

2.1.3 Cerebrovascular disease: The Epidemiology 9

2.1.4 Cerebrovascular Disease Risk Factors 9

2.1.5 Risk Prediction Assessment of Cardio-cerebrovascular by QRISK2 10

2.2 Cerebral small vessel disease (CSVD) 13

2.3 White matter hyperintensities (WMH) 16

2.4 Neuroimaging Modalities in Understanding of Heterogenous CSVD 20
2.4.1 Magnetic Resonance Imaging (MRI) 24
2.4.2 Basic principle of MRI 24
2.4.3 Application of MRI used to understand CSVD 26
2.4.4 Conventional MRI vs Advanced MRI 27
2.5 Diffusion Tensor Imaging (DTI) 27
2.5.1 DTI Theory to practice 30
2.5.2 Concepts of Diffusion in DTI 33
2.5.3 Quantitative DTI measures 35
2.5.4 DTI Analysis 37
2.5.5 Clinical application of DTI 38
2.6 DTI software 40
2.6.1 Type of software 40
2.6.2 Pipeline processing 44
2.7 Summary of Chapter 2 48
CHAPTER 3 METHODOLOGY 49
3.1 Ethic Approval and Funding 49
3.2 Sample Size Calculation and Estimation 49
3.3 Study Procedures 50
3.4 Subjects Recruitment and Cardiovascular Risk Prediction (QRISK2) 51
3.5 MRI Brain Scan Protocol 52
3.6 Phase I: Profiling of different DTI Software and pipeline processing 53
3.7 Phase II: Established Diffusion Tensor Imaging (DTI) Pipeline Processing 55
3.7.1 Pipeline Processing 1 (P1) 58
3.7.2 Pipeline Processing 2 (P2) 60
3.7.3 Pipeline Processing 3 (P3) 62
3.7.4 Pipeline Processing 4 (P4) 64
3.8 Phase III: Characterization of DTI pipeline processing 66

3.8.1 Comparison between the DTI pipeline processing 66

3.8.2 Determination of estimated total processing times in analyzing the DTI parameters. 68

3.8.3 Evaluation of DTI parameters in the WBT and ROI analysis in CSVD 69

3.8.4 Reliability Study of the pipeline processing 70

3.9 Statistical Analysis 70

3.10 Summary of chapter 3 71

CHAPTER 4 RESULTS 73

4.1 Subject Demography 73

4.2 Determination of DTI pipeline processing profile for white matter tractography analysis 74

4.3 Determination of user interface differences in DTI pipeline processing. 77

4.4 Comparison between the DTI pipeline processing for white matter tractography analysis 81

4.5 Determination of white matter lesion segmentation among MRI brain scans 83

4.6 Evaluation of DTI parameters in white matter tractography. 85

4.6.1 Whole Brain Tractography (WBT) Analysis 85

4.6.2 Region of Interest (ROI) Analysis 89

4.6.2(a) Right Anterior Corona Radiata (RACR) 89

4.6.2(b) Left Anterior Corona Radiata (LACR) 93

4.6.2(c) Right Superior Corona Radiata (RSCR) 97

4.6.2(d) Left Superior Corona Radiata (LSCR) 101

4.6.2(e) Right Superior Longitudinal Fasciculus (RSLF) 105

4.6.2(f) Left Superior Longitudinal Fasciculus (LSLF) 109

4.7 White Matter Integrity Comparison between WMH+ and WMH- 113

4.8 Reliability of DTI software pipelines 115

4.9 Summary of Chapter 4 115

CHAPTER 5 DISCUSSIONS 116

5.1 Introduction 116

5.2 Detection of WMHs 116
5.3 Characterization of DTI Pipeline Processing In CSVD. 117
5.4 Characterization of Tractography Parameter in CSVD. 119
5.4.1 WMHs Number of Lesion and Lesion Volume 119
5.4.2 Whole brain white matter tractography 122
5.4.3 Region of interest white matter tractography 122
5.4.4 Reliability of DTI software pipelines processing 125
CHAPTER 6 CONCLUSIONS 126
6.1 Limitation of study 127
6.2 Recommendation of future research 128
REFERENCE 129
APPENDICES 154

LIST OF TABLES

Table 2.1: Summary of the comparison between QRISK1 and QRISK2 (adapted from (Collins and Altman, 2010)..... 12

Table 2.2: Several cerebral small vessel disease (CSVD) manifestations according to STRIVE (Wardlaw *et al.*, 2013). 19

Table 2.3: Comparisons of different types of diagnostic modalities in the detection of CSVD – their advantages and disadvantages..... 21

Table 2.4: Schematic description of the main DTI parameters..... 35

Table 2.5: Software tools for DTI processing used in published studies (Hasan *et al.*, 2011; Soares *et al.*, 2013; Tromp, 2016)..... 42

Table 2.6: Steps available in software tools for DTI processing in published studies (Hasan *et al.*, 2011; Soares *et al.*, 2013; Tromp, 2016)..... 43

Table 2.7: Minimum requirement of data acquisition in DTI pipeline processing adapted from (Tanner and Stejskal, 1968). 45

Table 3.1: The inclusion and exclusion criteria for MRI brain scanning..... 51

Table 3.2: MRI sequence and acquisition protocols 52

Table 3.3: MRI sequence routinely used at Department of Radiology HUSM. 52

Table 3.4: List of keywords used in searching the research articles from the numerous databases between 2010 and 2017. 53

Table 3.5: List of inclusion and exclusion criteria in selecting the software as guided by related literature (Van Hecke and Emsell, 2016; van Norden *et al.*, 2012). 54

Table 3.6: Summary of pipeline processing methods for all the pipeline processing..... 57

Table 3.7: List of features determining the DTI software pipeline. 67

Table 3.8: Observation parameter (minutes)..... 68

Table 3.9: List of selected ROIs of WMH. 69

Table 4.1: A) Distribution of demographic variables in the study (n=60). 73

Table 4.2: Profile descriptions of DTI software pipeline processing..... 75

Table 4.3: Details features of all pipeline processing software.....78

Table 4.4: Relative scores based on features have in DTI software pipeline processing.....80

Table 4.5:The estimated total processing time, language implemented, strengths, and weaknesses of DTI software pipeline processing. 82

Table 4.6:Number and Volume of the lesion with WMH+ in 20 brains scan.....83

Table 4.7: Comparison of whole brain tractography (WBT) among subjects* with and without lesions in all sets of pipeline processing software. 86

Table 4.8: Significant means differences in whole brain tractography between with and without lesions in all sets of pipeline processing software. 87

Table 4.9: Changes of WBT parameters between all pipeline processing software. 88

Table 4.10: Comparison RACR among subjects with and without lesions in all sets of pipeline processing software.....90

Table 4.11: Significant means differences RACR between with and without lesions in all sets of pipeline processing software. 91

Table 4.12: Changes of RACR parameters between all pipeline processing software. 92

Table 4.13:: Comparison LACR among subjects with and without lesions in all sets of pipeline processing software.....94

Table 4.14: Significant means differences LACR between with and without lesions in all sets of pipeline processing software. 95

Table 4.15: Changes of LACR parameters between all pipeline processing software. 96

Table 4.16: Comparison RSCR among subjects with and without lesions in all sets of pipeline processing software.....98

Table 4.17: Comparison RSCR among subjects with and without lesions in all sets of pipeline processing software.....99

Table 4.18: Changes of RSCR parameters between all pipeline processing software.....100

Table 4.19: Comparison LSCR among subjects with and without lesions in all sets of pipeline processing software.....102

Table 4.20: Significant means differences LSCR between with and without lesions in all sets of pipeline processing software. 103

Table 4.21: Changes of LSCR parameters between all pipeline processing software. 104

Table 4.22: Comparison RSLF among subjects with and without lesions in all sets of pipeline processing software. 106

Table 4.23: Significant means differences RSLF between with and without lesions in all sets of pipeline processing software. 107

Table 4.24: Changes of RSLF parameters between all pipeline processing software. 108

Table 4.25: Comparison LSLF among subjects with and without lesions in all sets of pipeline processing software. 110

Table 4.26: Significant means differences LSLF between with and without lesions in all sets of pipeline processing software. 111

Table 4.27: Changes of LSLF parameters between all pipeline processing software 112

Table 4.28: Comparison between WMH^+ and WMH^- in white matter integrity 114

Table 4.29: Comparison between FA and MD value in WMH^+ subjects. 114

Table 4.30: The reliability test was conducted based on the DTI parameter in each of the pipelines. 115

Table 2.1: Summary of the comparison between QRISK1 and QRISK2 (adapted from (Collins and Altman, 2010) 12

Table 2.2: Several cerebral small vessel disease (CSVD) manifestations according to STRIVE (Wardlaw *et al.*, 2013). 19

Table 2.3: Comparisons of different types of diagnostic modalities in the detection of CSVD – their advantages and disadvantages. 21

Table 2.4: Schematic description of the main DTI parameters. 35

Table 2.5: Software tools for DTI processing used in published studies (Hasan *et al.*, 2011; Soares *et al.*, 2013; Tromp, 2016) 42

Table 2.6: Minimum requirement of data acquisition in DTI pipeline processing adapted from (Tanner and Stejskal, 1968). 45

Table 3.1: The inclusion and exclusion criteria for MRI brain scanning. 51

Table 3.2: MRI sequence and acquisition protocols 52

Table 3.3: MRI sequence routinely used at Department of Radiology HUSM. 52

Table 3.4: List of keywords used in searching the research articles from the numerous databases between 2010 and 2017. 53

Table 3.5: List of inclusion and exclusion criteria in selecting the software as guided by related literature (Van Hecke and Emsell, 2016; van Norden *et al.*, 2012). 54

Table 3.6: Summary of pipeline processing methods for all the pipeline processing. 57

Table 3.7: List of features determining the DTI software pipeline. 67

Table 3.8: Observation parameter (minutes). 68

Table 3.9: List of selected ROIs of WMH. 69

Table 4.1: A) Distribution of demographic variables in the study (n=60). 73

Table 4.2: Profile descriptions of DTI software pipeline processing. 75

Table 4.3: Details features of all pipeline processing software. 78

Table 4.4: Relative scores based on features have in DTI software pipeline processing. 80

Table 4.5:The estimated total processing time, language implemented, strengths, and weaknesses of DTI software pipeline processing. 82

Table 4.6:Number and Volume of the lesion with WMH+ in 20 brains scan. 83

Table 4.7: Comparison of whole brain tractography (WBT) among subjects with and without lesions in all sets of pipeline processing software. 86

Table 4.8: Significant means differences in whole brain tractography between with and without lesions in all sets of pipeline processing software. 87

Table 4.9: Changes of WBT parameters between all pipeline processing software. 88

Table 4.10: Comparison RACR among subjects with and without lesions in all sets of pipeline processing software. 90

Table 4.11: Significant means differences RACR between with and without lesions in all sets of pipeline processing software. 91

Table 4.12: Changes of RACR parameters between all pipeline processing software. 92

Table 4.13:: Comparison LACR among subjects with and without lesions in all sets of pipeline processing software. 94

Table 4.14: Significant means differences LACR between with and without lesions in all sets of pipeline processing software. 95

Table 4.15: Changes of LACR parameters between all pipeline processing software. 96

Table 4.16: Comparison RSCR among subjects with and without lesions in all sets of pipeline processing software. 98

Table 4.17: Comparison RSCR among subjects with and without lesions in all sets of pipeline processing software. 99

Table 4.18: Changes of RSCR parameters between all pipeline processing software 100

Table 4.19: Comparison LSCR among subjects with and without lesions in all sets of pipeline processing software. 102

Table 4.20: Significant means differences LSCR between with and without lesions in all sets of pipeline processing software. 103

Table 4.21: Changes of LSCR parameters between all pipeline processing software. 104

Table 4.22: Comparison RSLF among subjects with and without lesions in all sets of pipeline processing software. 106

Table 4.23: Significant means differences RSLF between with and without lesions in all sets of pipeline processing software. 107

Table 4.24: Changes of RSLF parameters between all pipeline processing software. 108

Table 4.25: Comparison LSLF among subjects with and without lesions in all sets of pipeline processing software. 110

Table 4.26: Significant means differences LSLF between with and without lesions in all sets of pipeline processing software. 111

Table 4.27: Changes of LSLF parameters between all pipeline processing software 112

Table 4.28: Comparison between WMH^+ and WMH^- in white matter integrity 114

Table 4.29: Comparison between FA and MD value in WMH^+ subjects. 114

Table 4.30: The reliability test was conducted based on the DTI parameter in each of the pipelines. 115

LIST OF FIGURES

Figure 2.1: Illustration of cerebral vasculature and general pathophysiology of CSVD. (A) Different branches of cerebral arteries and their territories supply cerebral white matter. (1) represent cortical arteries, (2) pial arterioles that supply deep white matter, (2.1) short branches, anterior choroidal arteries that branch into sub-ependymal arteries, arterioles of sub-ependymal, (5) MCA branches into thalamic and lenticulostriate perforating arteries that supply basal ganglia. (Martorell *et al.*, 2012) 15

Figure 2.2: MRI scanning is based on the excitation and relaxation of protons. Adapted from (Jones and Huber, 2018). 25

Figure 2.3: CSVD related lesion on MRI brain scanning. Changes related to CSVD with a summary of imaging characteristics of individual lesions with their MRI features. (DWI=diffusion-weighted imaging. FLAIR=fluid-attenuated inversion recovery. SWI=susceptibility-weighted imaging, GRE=gradient-recalled echo). Adapted from Wardlaw *et al.* (2013). 26

Figure 2.4: List features available in different DTI software packages. Adapted from Emsell and Sunaert (2016) 32

Figure 2.5: Illustration of hindered and restricted water inside and around boundaries. (e.g., cell membrane). Red dots (molecules are restricted by the presence of boundaries). Blue dots (molecules that are hindered by the presence of boundaries) 34

Figure 2.6: Typical DTI workflow. Adapted from (Soares *et al.*, 2013) 44

Figure 2.7: Formula for *b*-value. 46

Figure 2.8: Conceptual framework of this study. 48

Figure 3.1: General flowchart of the study. 50

Figure 3.2: Graphical user interface for FSL. The FDT diffusion utilised for Eddy Current Correction is shown in red (red arrowed). 58

Figure 3.3: General methods and steps for P1. 59

Figure 3.4: A) DSI studio's brain masking for skull stripping. (B) DSI studio's brain picture with computed diffusion tensor (note: depending on their diffusivity, different colours reflect distinct fibre orientation and direction.) 60

Figure 3.5: General methods and steps for P2. 61

Figure 3.6: A) Graphical user interface for Diffusion Toolkit. B) Graphical user interface for TrackVis. 62

Figure 3.7: General methods and steps for P3. 63

Figure 3.8: The DICOM data was uploaded and converted to a *.nrrd* file format using a 3D slicer. This is a graphical user interface for a 3D slicer. 64

Figure 3.9: General methods and steps for P4. 65

Figure 3.10: General flow of research carried out in this study. 72

Figure 4.1: Statistical probable WMHs voxels output from LST. A: Female, 44 years old without lesion (WMH^-). B: Male, 26 years old without lesion. C: Male, 26 years old with 1 lesion and lesion volume of 0.02 ml. D: Female, 42 years old with 5 lesions and lesion volume of 0.99 ml. (Note: images display is following neurological convention (Right on Right view). A red arrow indicated the lesion. 84

Figure 4.2: WBT from each of the P1 (A), P2 (B), P3 (C) and P4 (D). All the pictures are in the axial positions. Noted that red coloured tracts are the connecting fiber that connects between the left and right hemispheres. Blue coloured are the projection fibers that connect the brain to the spinal cord and supply to the whole body. The green colour tract is a commissural fiber the connect the posterior and anterior part of the brain. 85

Figure 4.3: (A) FLAIR MRI Brain image. (B)Statistical probable WMHs voxels output from LST signified the RACR lesion (red arrow). (C) RACR tract from P2 in axial position. (D) RACR region from P2 in axial position. (Notes: images display is following neurological convention – right on right view). 89

Figure 4.4: (A) FLAIR MRI Brain image. (B)Statistical probable WMHs voxels output from LST signified the LACR lesion (red arrow). (C) LACR tract from P2 in axial position. (D) LACR lesion from P2 in axial position. (Notes: images display is following neurological convention – right on right view). 93

Figure 4.5: (A) FLAIR MRI Brain image. (B)Statistical probable WMHs voxels output from LST signified the RSCR lesion (red arrow). (C) RSCR tract from P2 in axial position. (D) RSCR region from P2 in axial position. (Notes:

images display is following neurological convention – right on right view). 97

Figure 4.6: (A) FLAIR MRI Brain image. (B)Statistical probable WMHs voxels output from LST signified the LSCR lesion (red arrow). (C) LSCR tract from P2 in axial position. (D) LSCR region from P2 in axial position. (Notes: images display is following neurological convention – right on right view). 101

Figure 4.7: (A) FLAIR MRI Brain image. (B)Statistical probable WMHs voxels output from LST signified the RSLF lesion (red arrow). (C) RSLF tract from P2 in axial position. (D) RSLF region from P2 in axial position. (Notes: images display is following neurological convention – right on right view). 105

Figure 4.8: (A) FLAIR MRI Brain image. (B)Statistical probable WMHs voxels output from LST signified the LSLF lesion (red arrow). (C) LSLF tract from P2 in axial position. (D) LSLF region from P2 in axial position. (Notes: images display is following neurological convention – right on right view). 109

Figure 2.1: Illustration of cerebral vasculature and general pathophysiology of CSVD. (A) Different branches of cerebral arteries and their territories supply cerebral white matter. (1) represent cortical arteries, (2) pial arterioles that supply deep white matter, (2.1) short branches, anterior choroidal arteries that branch into sub-ependymal arteries, arterioles of sub-ependymal, (5) MCA branches into thalamic and lenticulostriate perforating arteries that supply basal ganglia. (Martorell *et al.*, 2012) 15

Figure 2.2: MRI scanning is based on the excitation and relaxation of protons. Adapted from (Jones and Huber, 2018). 25

Figure 2.3: CSVD related lesion on MRI brain scanning. Changes related to CSVD with a summary of imaging characteristics of individual lesions with their MRI features. (DWI=diffusion-weighted imaging. FLAIR=fluid-attenuated inversion recovery. SWI=susceptibility-weighted imaging, GRE=gradient-recalled echo). Adapted from Wardlaw *et al.* (2013). 26

Figure 2.4: List features available in different DTI software packages. Adapted from Emsell and Sunaert (2016) 32

Figure 2.5: Illustration of hindered and restricted water inside and around boundaries. (e.g., cell membrane). Red dots (molecules are restricted by the presence of boundaries). Blue dots (molecules that are hindered by the presence of boundaries).....34

Figure 2.6: Typical DTI workflow. Adapted from (Soares *et al.*, 2013) 44

Figure 2.7: Formula for *b*-value.....46

Figure 2.8: Conceptual framework of this study.....48

Figure 3.1: General flowchart of the study. 50

Figure 3.2: Graphical user interface for FSL. The FDT diffusion utilised for Eddy Current Correction is shown in red (red arrowed). 58

Figure 3.3: General methods and steps for P1. 59

Figure 3.4: A) DSI studio's brain masking for skull stripping. (B) DSI studio's brain picture with computed diffusion tensor (note: depending on their diffusivity, different colours reflect distinct fibre orientation and direction.) 60

Figure 3.5: General methods and steps for P2. 61

Figure 3.6: A) Graphical user interface for Diffusion Toolkit. B) Graphical user interface for TrackVis.....62

Figure 3.7: General methods and steps for P3. 63

Figure 3.8: The DICOM data was uploaded and converted to a *.nrrd* file format using a 3D slicer. This is a graphical user interface for a 3D slicer. 64

Figure 3.9: General methods and steps for P4. 65

Figure 3.10: General flow of research carried out in this study.....72

Figure 4.1: Statistical probable WMHs voxels output from LST. A: Female, 44 years old without lesion (WMH^-). B: Male, 26 years old without lesion. C: Male, 26 years old with 1 lesion and lesion volume of 0.02 ml. D: Female, 42 years old with 5 lesions and lesion volume of 0.99 ml. (Note: images display is following neurological convention (Right on Right view). A red arrow indicated the lesion. 84

Figure 4.2: WBT from each of the P1 (A), P2 (B), P3 (C) and P4 (D). All the pictures are in the axial positions. Noted that red coloured tracts are the connecting fiber that connects between the left and right hemispheres. Blue coloured are the projection fibers that connect the brain to the spinal cord and

supply to the whole body. The green colour tract is a commissural fiber the connect the posterior and anterior part of the brain. 85

Figure 4.3: (A) FLAIR MRI Brain image. (B)Statistical probable WMHs voxels output from LST signified the RACR lesion (red arrow). (C) RACR tract from P2 in axial position. (D) RACR lesion from P2 in axial position. (Notes: images display is following neurological convention – right on right view). 89

Figure 4.4: (A) FLAIR MRI Brain image. (B)Statistical probable WMHs voxels output from LST signified the LACR lesion (red arrow). (C) LACR tract from P2 in axial position. (D) LACR lesion from P2 in axial position. (Notes: images display is following neurological convention – right on right view). 93

Figure 4.5: (A) FLAIR MRI Brain image. (B)Statistical probable WMHs voxels output from LST signified the RSCR lesion (red arrow). (C) RSCR tract from P2 in axial position. (D) RSCR lesion from P2 in axial position. (Notes: images display is following neurological convention – right on right view). 97

Figure 4.6: (A) FLAIR MRI Brain image. (B)Statistical probable WMHs voxels output from LST signified the LSCR lesion (red arrow). (C) LSCR tract from P2 in axial position. (D) LSCR lesion from P2 in axial position. (Notes: images display is following neurological convention – right on right view). 101

Figure 4.7: (A) FLAIR MRI Brain image. (B)Statistical probable WMHs voxels output from LST signified the RSLF lesion (red arrow). (C) RSLF tract from P2 in axial position. (D) RSLF lesion from P2 in axial position. (Notes: images display is following neurological convention – right on right view). 105

Figure 4.8: (A) FLAIR MRI Brain image. (B)Statistical probable WMHs voxels output from LST signified the LSLF lesion (red arrow). (C) LSLF tract from P2 in axial position. (D) LSLF lesion from P2 in axial position. (Notes: images display is following neurological convention – right on right view). 109

LIST OF ABBREVIATION

3D	:	3 Dimensional
ACR	:	Anterior Corona Radiata
AD	:	Axial Diffusivity
ADC	:	Apparent Diffusion Coefficient
ALS	:	Amyotrophic Lateral Sclerosis
ASEAN	:	Association of Southeast Asian Nations
CC	:	Carpus Callosum
cMRI	:	Conventional Magnetic Resonance Imaging
CSVD	:	Cerebral Small Vessel Disease
CT	:	Computed Tomography
CTA	:	Computed Tomography- Angiography
DALYs	:	Disability Adjusted Living Years
D	:	Diffusion Tensor
dMRI	:	Diffusion MRI
DTI	:	Diffusion Tensor Imaging
DTT	:	Diffusion Tensor Tractography
DWI	:	Diffusion-Weighted Imaging
EPI	:	Echo Planar Imaging
FA	:	Fractional Anisotropy
FACT	:	Fiber Assignment by Continuous Tracking
FDT	:	FSL Diffusion Toolbox
FLAIR	:	Functional Attenuated Inversion Recovery
fMRI	:	Functional Magnetic Resonance Imaging
FOV	:	Field of View
FSL	:	Functional Magnetic Resonance Imaging of The Brain Software Library

FT	:	Fiber Tracking
GUI	:	Graphical User interfaces
HARDI	:	High Angular Resolution Diffusion Imaging
HUSM	:	Hospital Universiti Sains Malaysia
IDL	:	Interface Design Language
JEPeM-USM	:	Jawatan Kuasa Penyelidikan Manusia @ USM Human Ethics Committee
JHU	:	John Hopkins University
JPEG	:	Joint Photographic Expert Group
LACR	:	Left Anterior Corona Radiata
LGA	:	Lesion Growth Algorithm
LSCR	:	Left Superior Corona Radiata
LSLF	:	Left Superior Longitudinal Fasciculus
LST	:	Lesion Segmentation Tools
LV	:	Lesion Volume
MATLAB	:	Matrix Laboratory
MCA	:	Middle Cerebral Arteries
MCI	:	Mild Cognitive Impairment
MD	:	Mean Diffusivity
ml	:	Millilitre
mm	:	Millimetre
mT	:	MilliTesla
MRA	:	Magnetic Resonance Angiography
MRI	:	Magnetic Resonance Imaging
NHMS	:	National Health and Morbidity Survey
NIfTI	:	Neuroimaging Informatics Technology Initiative
NLLS	:	Non-Linear Least Square
NOL	:	Number of Lesions

NOT	:	Number of Tracts
OLS	:	Ordinary Least Square
PET	:	Positron Emission Tomography
PCT	:	Perfusion Computed Tractography
PLIC	:	Posterior Limb of Internal Capsule
QRISK2	:	Cardiovascular Risk Prediction Score
RACR	:	Right Anterior Corona Radiata
RD	:	Radial Diffusivity
RF	:	Radio Frequency
ROI	:	Region of Interest
RSCR	:	Right Superior Corona Radiata
RSLF	:	Right Superior Longitudinal Fasciculus
SCR	:	Superior Corona Radiata
SD	:	Standard Deviation
SENSE	:	Sensitivity Encoding
SLF	:	Superior Longitudinal Fasciculus
SPM12	:	Statistical Parametric Mapping Version 12
SPSS	:	Statistical Package for The Social Science
STRIVE	:	Standard for Reporting and Imaging of Small Vessel Disease
SVD	:	Small Vessel Disease
TBSS	:	Tract-Based Spatial Statistics
T	:	Tesla Unit
TE	:	Echo Time
TIA	:	Transient Ischaemic Attack
TI	:	Inversion Time
TL	:	Tract Length
TR	:	Repetition Time

Tr	:	Trace
VaD	:	Vascular Dementia
VCI	:	Vascular Cognitive Impairment
VBA	:	Voxel-Based Analysis
WBT	:	Whole Brain Tractography
WHO	:	World Health Organisation
WLLS	:	Weighted Linear Least Squares
WM	:	White Matter
WMI	:	White Matter Integrity
WML	:	White Matter Lesion
WMH	:	White Matter Hyperintensities

LIST OF APPENDICES

Appendix A	Determination of processing times in analysing the DTI parameters
Appendix B	Ethical Approval
Appendix C	Ethical Extension Approval
Appendix D	Consent Form – Bahasa Malaysia
Appendix E	Consent Form – English

ABSTRAK

KAJIAN PIPELIN TRAKTOGRAFI BERBEZA DALAM PEMBULUH DARAH KECIL INDIVIDU ASIMPTOMATIK DENGAN PENYAKIT PEMBULUH DARAH KECIL OTAK

Pendahuluan: Penyakit pembuluh darah kecil otak (CSVD) sering ditemui sebagai penemuan asimptomatik (‘senyap’) pada pengimbasan otak menggunakan Pengimejan Resonans Magnetik (MRI). MRI berasaskan difusi, seperti pengimejan tensor resapan (DTI), adalah teknik neuropengimejan yang muncul untuk mengesan dan menilai manifestasi CSVD, seperti hiperintensiti jirim putih (WMHs). DTI telah digunakan secara progresif, tetapi tiada standard emas untuk mengoptimumkan pemprosesan pipelin DTI, terutamanya dalam kajian CSVD. Oleh itu, untuk memanfaatkan DTI dengan sebaiknya, beberapa pertimbangan teknikal dan metodologi mesti dibuat.

Objektif: Matlamat kajian ini adalah untuk mewujudkan satu siri pemprosesan pipelin DTI sama ada dalam satu atau gabungan beberapa pakej perisian yang mapan untuk mengkaji keserasian, kebolehulangan, dan kebolehpercayaan dalam penilaian integriti iskemia jirim putih dalam CSVD tanpa gejala.

Kaedah: Enam puluh (n = 60) orang peserta yang tanpa gejala (purata umur, 39.82 ± 11.32) telah direkrut dan diimbas dengan pengimbas MRI 3T. Dua puluh (n = 20) peserta mempunyai WMH. Empat pemprosesan pipelin telah ditubuhkan, iaitu: P1 (MedINRIA), P2 (DSI Studio), P3 (DTI Toolkit dan TrackVis), dan P4 (3Dslicer).

Hasil kajian: Setiap profil pemprosesan pipelin DTI dan perbezaan antara muka pengguna telah dibincangkan, termasuk bahasa pengaturcaraan yang digunakan, anggaran jumlah masa pemprosesan, kekuatan dan kelemahan mereka. Perbandingan antara setiap pemprosesan pipelin DTI memberitahu bahawa P2 adalah yang terbaik antara pemprosesan

pipelin lain yang digunakan dalam kajian ini kerana mempunyai skor relatif perbezaan antara muka pengguna yang tinggi. P2 juga mempunyai skor kebolehpercayaan yang baik ($\alpha = 0.86$).

Kesimpulan: Kajian ini membuktikan keserasian, kebolehulangan, dan kebolehpercayaan pipelin DTI yang mapan dalam penilaian integriti iskemia jirim putih dalam CSVD tanpa gejala. Ia menyediakan analisis komprehensif yang boleh menambah baik dan menyeragamkan pengenalpastian WMH dan membolehkan penilaian integriti bahan putih yang lebih mantap. Penemuan kami menunjukkan bahawa skor kebolehpercayaan yang boleh diterima dalam pemprosesan paip DTI adalah P2 (DSI Studio), yang dapat berfungsi sebagai pemprosesan pipelin yang ideal untuk menilai tractografi bahan putih dalam CSVD .

ABSTRACT

DIFFERENTIAL TRACTOGRAPHY PIPELINES STUDY IN ASYMPTOMATIC INDIVIDUALS WITH CEREBRAL SMALL VESSEL DISEASE

Introduction: Cerebral small vessel disease (CSVD) is frequently discovered as an asymptomatic ('silent') finding during magnetic resonance imaging (MRI) brain scanning. Diffusion-based MRI, such as diffusion tensor imaging (DTI), is an emerging neuroimaging technique to detect and evaluate the CSVD manifestations, such as white matter hyperintensities (WMHs). DTI has been used progressively, but there is no gold standard for optimising the DTI pipeline processing, especially in the CSVD study. Therefore, to make the best use of DTI, several technical and methodological considerations must be made.

Objective: The goal of this study is to establish a series of DTI pipeline processing either in a single or a combination of multiple well-established software packages in order to study their compatibility, reproducibility, and reliability in the assessment of white matter ischaemic integrity in asymptomatic CSVD.

Methods: Sixty (n = 60) asymptomatic people (mean age, 39.82 years old ± 11.32) were recruited and had their brains scanned with a 3T MRI scanner. Twenty (n = 20) of the participants had WMHs. Four pipeline processing were established: P1(MedINRIA), P2 (DSI Studio), P3 (DTI Toolkit and TrackVis), and P4 (3Dslicer).

Results: Each established DTI pipeline processing profile and user interface differences were discussed, including the programming language used, estimated total processing times, and their strengths and weaknesses. The comparison between each of the DTI pipelines processing was determined to be P2 as the best among the other pipelines processing used in this study based on the highest relative score of user interface differences. P2 also has a good reliability score ($\alpha = 0.86$).

Conclusion: This study established the compatibility, reproducibility, and reliability of established DTI pipelines in the assessment of white matter ischemic integrity in apparently asymptomatic CSVD. It provides a comprehensive analysis that can improve and standardise the identification of WMHs and allow for a more robust white matter integrity assessment. Our findings show that the acceptable reliability score in the established DTI pipelined processing is P2 (DSI Studio), which can serve as an ideal pipeline processing to assess white matter tractography in CSVD.

CHAPTER 1

INTRODUCTION

1.1 Introduction

Cerebral small vessel disease (CSVD) is recognised as a significant reason for age-related vascular cognitive impairment, causing major disability and decreased personal satisfaction (Zeestraten *et al.*, 2016). CSVD can be regarded as a neurovascular syndrome featuring clinical, cognitive, neuroimaging, and neuropathological findings that arise from damage to arterioles, small arteries, vessels, small veins and venules in the brain (Li *et al.*, 2018a; Moody *et al.*, 1995; Sorond *et al.*, 2015). CSVD is commonly referred as to a series of neuroimaging (i.e., magnetic resonance imaging [MRI]) variations, consisting of recent small subcortical infarcts, lacunes, white matter hyperintensities (WMHs), cerebral microbleeds (CMBs), prominent or enlarged perivascular spaces (ePVS), cortical microinfarcts, and atrophy (Che Mohd Nassir *et al.*, 2021; Litak *et al.*, 2020; Shi and Wardlaw, 2016). Recent small subcortical infarcts normally cause acute stroke symptoms, while other CSVD lesions are clinically more subtle and thus described as "silent" lesions (Das *et al.*, 2019). In the silent CSVD manifestation, the diagnosis is made through the incidental finding from neuroimaging that is regularly utilised as a diagnosis marker after a first suggestive CSVD appearance (Mustapha *et al.*, 2019).

On conventional brain imaging such as computed tomography (CT) scans, or hyperintensity on T2-weighted MRI, this common manifestation of CSVD appears ill-defined. While conventional MRI and MRI-based diffusion-weighted imaging (DWI) provide a detailed picture of the overall severity of white matter involvement, it is only capable of measuring diffusion in one direction. Therefore, improved relationships and reliable lesion studies are

needed to enhance the assessment of white matter architecture and connectivity, such as white matter tractography using diffusion-based MRI (dMRI) (Lee *et al.*, 2015; Nitkunan *et al.*, 2008).

Within dMRI, diffusion tensor imaging (DTI) is a signal modelling technique. Through fiber tracking (FT), DTI can offer data that can be used to explain brain white matter connections non-invasively (Chen and Song, 2008; Ouyang *et al.*, 2015). FT is a three dimensions (3D) reconstruction method to evaluate neural tracts using data collected by DTI. DTI can measure diffusion in 3D, which evaluates the anisotropy of water diffusion in brain tissues and gives an indication of damaged white matter (Foerster et al., 2014; Tha et al., 2010). Fractional anisotropy (FA), mean diffusivity (MD), radial and axial diffusivity (RD and AD) are some of the diffusion parameters used in DTI analysis to determine white matter integrity (Nagesh et al., 2008; Tha et al., 2010). Any changes in these parameters provide insight into the properties of specific white matter in connection to specific disorders, such as WMHs. However, the physiological underpinnings of changes in these parameters are not known.

One of the more current improvements in DTI is the advancement of models of individual patient-specific white matter tracts, which is diffusion tensor tractography (DTT), suited to examine the effect of CSVD on white matter tracts. DTT enables the creation of a white matter tract model, and the effects of a CSVD lesion on the integrity of these tracts can be described. Recent studies have used tractography techniques to identify the proximity of infarcted tissue to major white matter tracts. Because of this newer development, its full impact on the study of CSVD has not been realised (Davis et al., 2009; Zeestraten et al., 2016). A pipeline is a connected series of image processing elements, in which the output becomes the input of the next image processing unit in a pipeline.

Although a lot of research has been reported using DTI analysis in CSVD, there is no standardisation technique for choosing a specific pipeline for DTI analysis. This is because most of the research teams are using their own and different combinations of software in their pipelines, especially in the study of the onset and progression of silent CSVD. Hence, we

examined DTI pipeline processing on CSVD to uncover a better analysis method for assessing the white matter integrity of CVSD. This is due to a poor diagnosis method that is dependent on incidental findings through neuroimaging brain scans. Therefore, this study aimed to develop or establish a series (or several) of DTI pipeline processing either in single or combination of multiple well-established software, hence, to study their compatibility, reproducibility, and reliability in the assessment of white matter ischaemic integrity in asymptomatic CSVD.

1.2 Rationale and Significance of Study

A "silent" or "asymptomatic" CSVD manifestation is regularly perceived as a coincidental result of neuroimaging and is frequently utilised as a prognostic sign. Advancements in neuroimaging (MRI) methods may provide new insights into illness pathomechanism with alternate indicators of disease onset, progression, and therapy assessments. Recent advancements in dMRI (i.e., DTI) provide a better understanding of white matter integrity in healthy and asymptomatic people and thus might be used as a possible signal of CSVD onset and development. The goal of this study is to discover better analysis techniques for the identification of CSVD, particularly in asymptomatic individuals. Is it possible that the specific DTI pipeline processing software may be useful in detecting asymptomatic CSVD?

1.3 Objectives

1.3.1 General Objective

To establish a series of DTI pipeline processing either in single or combination of multiple well-established software in order to study their compatibility, reproducibility, and reliability in the assessment of white matter ischaemic integrity in asymptomatic CSVD.

1.3.2 Specific Objectives

1. To determine the profile of different DTI software and pipeline processing used for the white matter tractography analysis.
2. To compare the profile of the established DTI pipelines processing used for the white matter tractography analysis.
3. To determine the user interface differences in each of the established DTI pipeline processing.
4. To characterize the reproducibility of the established DTI pipeline processing parameters (FA, MD, tract length) for white matter tractography analysis (whole brain and region of interest, ROI).
5. To determine the reliability of each of the established DTI pipeline processing.

1.3.3 Research Question

1. Do different software packages give different fibers tracking result/s?

2. Do different combinations of software and pipelines give different tractography parameters of white matter tract of interest?

3. Will differences in utility and reliability of different combinations of software and pipelines give different output/s in the assessment of WMHs?

1.3.4 Research Hypothesis

1. Different software packages and pipelines processing could potentially give different output because of various settings issued during data acquisition and several algorithms used to perform the fiber tracking.

2. Differences in DTI parameters (FA, MD) when compared to the different combinations of software pipelines.

3. There might also have differences in the utility and reliability in this different combination of software pipeline processing as an assessment of WMHs in asymptomatic CSVD.

CHAPTER 2

LITERATURE REVIEW

2.1 Introduction to cerebrovascular disease

2.1.1 Definition & Classification

"Cerebrovascular disease" is a relatively new word. Initially, it was recorded in the 8th edition of the International Classification of Diseases (ICD 8) in 1965 (World Health, 1967), where it is classified as a circulatory condition apart from nervous system diseases. Cerebrovascular is composed of two sections: "Cerebro" describes brain major section, and "vascular" describes veins and arteries. Blood flow in the brain is referred to as cerebrovascular (Archie and Cucullo, 2019). Cerebrovascular disease is defined as any illness in the brain region that is momentarily or permanently damaged by ischemia or bleeding, and one or more cerebral blood vessels are implicated in the pathological process (Millikan *et al.*, 1975; Sacco *et al.*, 2013).

The term "stroke" is commonly used to connect these concepts. Haemorrhagic (further divided according to location as intracerebral, subdural, or subarachnoid), ischemic, and lacunar stroke, all characterised by their morbid pathology, and transient ischemic attack (TIA), defined by its clinical presentation, are among the subgroups covered by the word “stroke” (Filippi and Rocca, 2020; Keselman, 2021). These sub-types are thought to be caused by a range of pathophysiological processes. All strokes are known to occur from a disruption of the brain's vascular supply. As a result, the terms "stroke" and "cerebrovascular illness" have become interchangeable (Storey and Pols, 2009). Stroke, intracranial stenosis, vertebral stenosis, carotid stenosis, aneurysms, and vascular abnormalities are all examples of cerebrovascular illness.

2.1.2 Types of cerebrovascular disease

25% of ischaemic strokes (infarction) happen due to intracranial small vessel disease (Feinberg *et al.*, 1996; Norrving, 2008). Thrombotic cerebral infarction happens due to the atherosclerotic barrier of huge arteries, with occluded in the whole or part of the artery which results in obstruction at the primary atherosclerotic lesion or in embolism at other distal arteries (Behrouzi and Punter, 2018; Murphy and Werring, 2020). An embolic cerebral infarction occurs because of the embolism of a clot within the cerebral arteries returning from alternative parts of the arterial system (i.e., from internal organ lesions). It is either at the location of the valves or of the heart cardiac cavities or because of rhythm disturbances with stasis of the blood, that permits clotting within the heart, as seen in atrial fibrillation (Murphy and Werring, 2020). Lacunar cerebral infarctions are one part of the CSVD spectrum, are small deep infarcts around the territory of small penetrating arteries that happen because of neighbouring disease of these vessels, generally associated with recurring high blood pressure (Abdurakhmanov, 2021; Harris *et al.*, 2018; Nair *et al.*, 2021).

A short-term cerebrovascular episode that leaves no lasting injury and lasts less than 24 hours is known as a transient ischemic attack (TIA). Presumably, there is a blockage in an artery of the brain, triggering stroke-like signs, but the obstruction clears sooner than any long-lasting damage happens. A warning sign of TIA resolves quickly, although the symptoms may be like strokes. It is so ambiguous that people simply ignore it (particularly when it lasts barely a few minutes) (Murphy and Werring, 2020). Spontaneous intracerebral haemorrhage is primarily caused by arteriolar hypertensive illness and rarely because of clotting syndromes, vascular abnormalities inside the brain, and diet (i.e., extreme liquor intake, low blood cholesterol fixation, hypertension, and so on) (An *et al.*, 2017). Cortical amyloid angiopathy (an effect of high blood pressure) could be a reason behind cortical haemorrhages, particularly happening in aged individuals (Malek-Ahmadi *et al.*, 2019).

2.1.3 Cerebrovascular disease: The Epidemiology

Around the world, cerebrovascular diseases such as stroke are another common reason for death and the primary cause of adult disability (Feigin *et al.*, 2016). Globally, around 15 million individuals a year are diagnosed with stroke. The aforesaid, 5 million pass and another 5 million are forever incapacitated (Asri *et al.*, 2020). Death rates from stroke fluctuate across the globe, with a ten-times variation in age-changed death rates and Disability-Adjusted Living Years (DALYs) lost between the uppermost and lowest most positioned countries. Nationwide revenue was a specific solid indicator of stroke burden and death (Mukherjee and Patil, 2011; Tetzlaff *et al.*, 2020). Death rates were 3.5 times higher in low-salary countries than in middle-salary countries (Feigin *et al.*, 2014; Johnston *et al.*, 2009). In ASEAN countries, stroke is in the top four important causes of death, ranging from 10.9/100,000 people in Thailand to 54.2/100,000 people in Singapore (Feigin *et al.*, 2016; Katan and Luft, 2018).

Shu *et al.* (2019) show that small vessel infarction or lacunar infarcts occur less often in Caucasians compared to Asians (Ng *et al.*, 1996; Wolma *et al.*, 2009). Based on the Ministry of Health statistics, stroke has been in the top five important causes of death in Malaysia since the 2000s. Data in 2009 shows cerebrovascular disease causing the death of 8.43/100,000 residents. The occurrence of stroke in 2006 was predictable to be 0.3% among Malaysians during the third National Health and Morbidity Survey (NHMS). The identical assessment showed the elevated incidence of stroke between individuals single (0.1%) and married (0.9%) compared to divorced or widowed (2.5%) (Loo and Gan, 2012). Stroke could either be ischemic or haemorrhagic disruptions of the cerebral blood circulation (Lauritzen *et al.*, 2011).

2.1.4 Cerebrovascular Disease Risk Factors

In 1960, The Framingham Heart Study was the first to identify non-changeable and changeable risk factors for cerebrovascular illness in general people (Ezennaka and Dodiyi-Manuel, 2021; Mahmood *et al.*, 2014). Understanding such variables has aided in the diagnosis and treatment of cardiovascular morbidity and death. Age, ethnicity, gender, race, and genetics is prevalent nonmodifiable cause for stroke (Palomeras Soler and Casado Ruiz, 2010). While

these variables cannot be changed, they do assist in identifying people who are at high risk, allowing for strategic treatment of modifiable causes like cholesterol levels and smoking.

Moreover, it has been stated that the probability of having a stroke doubles every ten years beyond the age of 55 for both males and females (Gallù *et al.*, 2020; Shihmanter *et al.*, 2021). Similarly, men have a 1.25 times greater incidence of stroke compared to women, owing to women living longer lives(Choudhury *et al.*, 2015). Stroke incidence and death rates vary significantly by race. Previous research found that the incidence of stroke in black and Hispanic individuals is double that of white people (Boden-Albala et al., 2019; Ramirez et al., 2016; Stamos and Darbar, 2016). Asians, such as Chinese and Japanese, have a higher incidence of stroke (Chiang et al., 2014).

Furthermore, those with a family history of stroke have a higher incidence and prevalence of stroke. This is due to shared familial exposure to environmental or lifestyle risk, a genetic tendency for stroke, and a genetic determination of additional stroke risk factors. Earlier research indicated that males whose moms died from stroke and females with a family history of stroke were more likely to have one (Samai *et al.*, 2015). It also indicated that both paternal and maternal stroke history increased the risk of stroke (Tian *et al.*, 2017).

2.1.5 Risk Prediction Assessment of Cardio-cerebrovascular by QRISK2

At present, an online calculator has been developed to estimate the risk of cardiocerebrovascular illness over the next ten years; this tool is known as QRISK 2. (Collins and Altman, 2010). QRISK2 (https://qrisk.org/) is an online risk prediction tool for cardiocerebrovascular illness developed by the University of Nottingham and EMIS, United Kingdom (UK) and based on data from over 10 million patients enrolled with 550 general practitioners in the country between 1993 and 2010. As a result, it is widely used across the world and is updated every year.

QRISK2 is an improved version of QRISK1, with a new nonlinear system risk score that incorporates all the lifestyle factors from QRISK1, including self-allocated background and

symptoms related to cardiocerebrovascular risks, such as hypertension, type 2 diabetes mellitus, atrial fibrillation, rheumatoid arthritis, and renal disease (Hippisley-Cox *et al.*, 2008). QRISK2 considers relationships between age and BMI, family history, systolic blood pressure, treated hypertension, smoking status, atrial fibrillation, and diagnosed type 2 diabetes mellitus (Table 2.1).

Table 2.1: Summary of the comparison between QRISK1 and QRISK2 (adapted from (Collins and Altman, 2010)

QRISK1
• Age (continuous) • Ratio of total serum cholesterol: high-density lipoprotein (continuous) • Systolic blood pressure (continuous) • Smoking status (current smoker/non-smoker (including former smoker)) • Body mass index (continuous) • Family history of coronary heart disease in first-degree relative under 60 years (yes/no) • Townsend deprivation score (output area level 2001 census data evaluated as a continuous variable) • Receiving treatment for blood pressure at baseline (at least one current prescription of at least one antihypertensive agent) (yes/no) • Systolic blood pressure × Receiving treatment for blood pressure at baseline
QRISK2
• Age (continuous) • Ratio of total serum cholesterol: high-density lipoprotein (continuous) • Systolic blood pressure (continuous) • Smoking status (current smoker/non-smoker (including former smoker)) • Body mass index (continuous) • Family history of coronary heart disease in first-degree relative under 60 years (yes/no) • Townsend deprivation score (output area level 2001 census data evaluated as a continuous variable) • Treated hypertension (diagnosis of hypertension and at least one current prescription of at least one antihypertensive agent) (yes/no) • Self-assigned ethnicity (white (or not recorded) /Indian/Pakistani/ Bangladeshi/) /Indian/Pakistani/Bangladeshi/another Asian/black African/Black Caribbean/other (including mixed)) • Type 2 diabetes (yes/no) • Rheumatoid arthritis (yes/no) • Atrial fibrillation (yes/no) • Renal disease (yes/no) • Age × body mass index • Age × Townsend score • Age × systolic blood pressure • Age × family history of cardiovascular disease • Age × smoking current • Age × treated hypertension • Age × type 2 diabetes • Age × atrial fibrillation

2.2 Cerebral small vessel disease (CSVD)

Currently, the cardiocerebrovascular disease is the most prominent cause of death and disability (Mensah *et al.*, 2019). Both the heart and the brain show parallel vascular anatomy, with enormous conduit arteries running on the surface of the organ, supplying tissue perfusion through a complex system of penetrating small vessels. Both organs depend on the delicate change in local blood flow to match metabolic requirements. Blood flow regulation needs sufficient functioning of the microcirculation in both organs, with failure of microvascular function, termed small vessel disease (SVD), causing various possible clinical manifestations (Berry *et al.*, 2019; Moroni *et al.*, 2020).

In the brain, CSVD can trigger an acute stroke disease recognized as lacunar stroke or additional insignificant pathological changes in the brain parenchyma, which sooner or later cause neurological deficits or cognitive weakening (Cuadrado-Godia *et al.*, 2018). Coronary microcirculation cannot be pictured in vivo in people, and practical data can be deduced by assessing the coronary flow reserve. Common brain lesions detected through MRI findings related to CSVD include small subcortical infarcts, white matter hyperintensities, lacunes, perivascular spaces, and cerebral microbleeds. There is proof that such structural alterations indicate underlying CSVD (Wardlaw *et al.*, 2013).

Blood supply comes from two main pairs of arteries in the brain, which are the internal carotid artery and the vertebral artery on each side (Mai *et al.*, 2016). When blockage (ischaemia) happens in the blood vessels in the brain, it can cause symptomatic or asymptomatic cerebral small vessel disease (CSVD). Figure 2.1 illustrate the general pathophysiology of CSVD. Pathological conditions affecting the small vessels of the brain and resulting in CSVD have indicated plausible molecular mechanisms involved in vascular impairment and their effect on brain function and cognitive decline (Østergaard *et al.*, 2015; Rincon and Wright, 2014). Ischaemic strokes are one type of stroke that results from blockage (ischaemic) of a small end artery inside the brain (Rouhl. *et al.*, 2009). Around 10% to 30% of ischaemic strokes or

lacunar strokes are represented by CSVD (Heye *et al.*, 2015; Patel and Markus, 2011; Rouhl. *et al.*, 2009).

CSVD is a brain injury that badly collateralizes grey and deep white matter in the subcortical area because of various vascular-pathologic developments that cause obstruction to the perforating cerebral capillaries and arteries that enter and provide the brain subcortical region (Benjamin *et al.*, 2015; Hinman *et al.*, 2015; Novakovic, 2010). CSVD affect neuropsychological function, and common neuropathological processes and has an important role in cognitive impairment, dementia, and stroke (Gong *et al.*, 2015; Heye *et al.*, 2015; Lambert *et al.*, 2015; Nitkunan *et al.*, 2008).

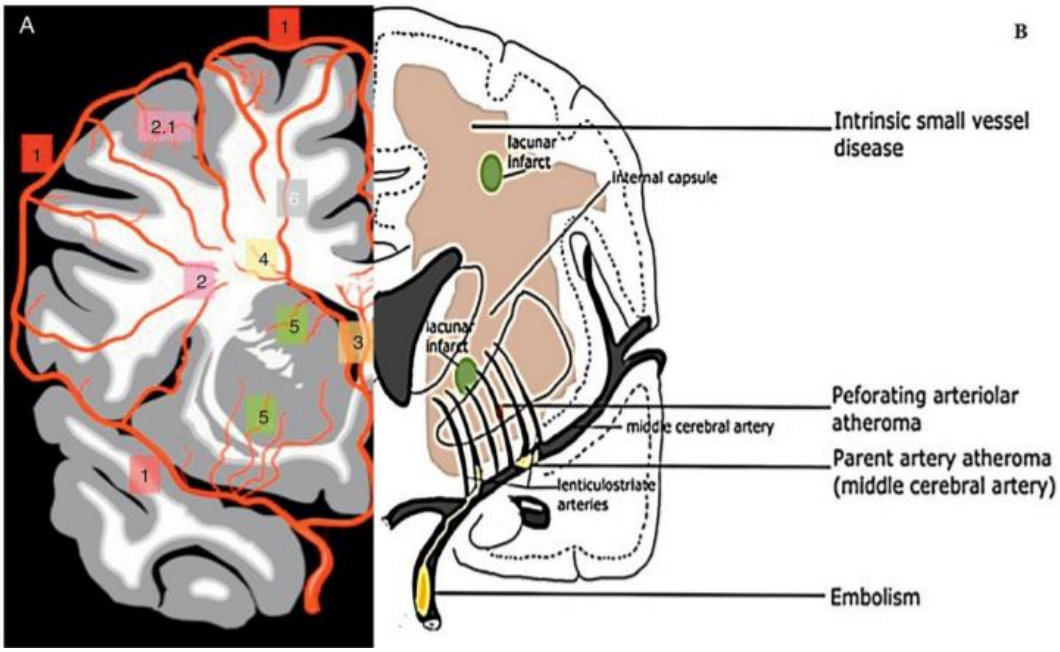

Figure 2.1: Illustration of cerebral vasculature and general pathophysiology of CSVD. (A) Different branches of cerebral arteries and their territories supply cerebral white matter. (1) represent cortical arteries, (2) pial arterioles that supply deep white matter, (2.1) short branches, anterior choroidal arteries that branch into sub-ependymal arteries, arterioles of sub-ependymal, (5) MCA branches into thalamic and lenticulostriate perforating arteries that supply basal ganglia. (Martorell *et al.*, 2012)

B) The picture shows branches of MCA that penetrates the subcortical region of white matter and grey matter. An embolism goes up to MCA and ends up entering and occluding lenticulostriate arteries, resulting in a lacunar lesion in basal ganglia. If the atheroma in the parent artery is positioned at the opening of its penetrating branches, it could lead to an acute occlusion of one or several penetrating arteries hence causing a lacunar infarct. Intensive small vessel disease may lead to the diffused disrupted blood-brain barrier. MCA, middle cerebral arteries (Shi and Wardlaw, 2016).

2.3 White matter hyperintensities (WMH)

White matter hyperintensities (WMHs) are among the most important and regularly encountered alterations in MRI brain scanning. On neuroimaging, WMHs occur as regions of signal hyperintensity scattered within the deep and periventricular white T2-weighted or Fluid-attenuated inversion recovery (FLAIR) pictures (Wardlaw *et al.*, 2015). WMHs can be found in MRI images of asymptomatic people, and their incidence increases with time. Their occurrence is much higher in people with a background of cardiovascular risk factors, proven cardiovascular disease, or renal impairment (Schmahmann *et al.*, 2008). WMHs have been linked with an overall deterioration of superior functions, along with an increase in stroke, dementia, and mortality. A high burden of WMHs has been correlated with gait disturbance and the risk of falls, including urinary symptoms, which cause an increase in overall disability and dependency (Li *et al.*, 2017).

MRI can identify the ischemic repercussions of various CSVD manifestations (Table 2.2) including WMHs, cerebral microbleeds, lacunar strokes, increased perivascular gaps, and tiny subcortical infarcts (Zhao *et al.*, 2020). On FLAIR and T2-weighted MRI characteristics, WMHs are often identified as tiny 'lacunes' (lake in Latin) in the ageing brain or brilliant regions of small non-cavitated high signal intensity. The lesions will worsen with age, as they progress throughout a few months to years (Benjamin *et al.*, 2018; Ghaznawi *et al.*, 2019). Wardlaw *et al.* (2013), have developed the neuroimaging standard for research in visual identification and categorization of CSVD spectrum recognized as Standards for Reporting and Imaging of Small Vessel Disease (STRIVE).

WMHs are a type of white matter ischemia that can manifest either as symptomatic or asymptomatic brain lesions. This can be identified as incidental findings from patients brain imaging that never had any symptoms of stroke and is most common in the elderly (Valdés Hernández *et al.*, 2015). This has also been used as a predictive indicator for symptomatic CSVD, such as acute lacunar stroke (van Norden *et al.*, 2011).

Lacunar infarcts (observed as WMHs on neuroimaging) account for around 95 percent of asymptomatic or silent brain infarction (SBI) and are more common than symptomatic infarcts. Age and hypertension are two significant factors that contribute to the development of SBI (Norrving, 2015). Location and magnitude are the primary distinctions between SBI and symptomatic lacunar infarctions due to both pathological similarities (Bailey *et al.*, 2012). For example, asymptomatic SBI is usually seen in the periventricular region and centrum semiovale of white matter (Kaiser *et al.*, 2014; Wharton *et al.*, 2015), while symptomatic lacunar ischaemic stroke mainly changes the sensory and motor pathways (Valdés Hernández *et al.*, 2015).

Nevertheless, the fundamental pathomechanism of SBI or WMHs remains a point of contention, due to discoveries from histopathological, epidemiological, and physiological investigations that provide crucial information. Furthermore, healthy white matter is more myelinated compared to Alzheimer's patients (Bartzokis *et al.*, 2003), which has a high concentration of long-chain fatty acids and has less water (by 12%) than grey matter. WMHs are consistently associated with age, hypertension, and other cardiovascular risk factors (Zhao *et al.*, 2019). Individuals that have substantial WMHs have a greater risk of a potential stroke, indicating that WMHs can be used as a prognostic indicator. Nonetheless, SBI or WMHs is believed to affect about 30% of healthy people over the age of 60 (de Leeuw *et al.*, 2001; Hilal *et al.*, 2017).

Brain atrophy is connected to reduced blood flow to the brain and localised cognitive symptoms, which is linked to the quantity and size of WMHs (van Dalen *et al.*, 2016). Additionally, WMHs are linked to vascular cognitive impairment and related to the development of neuropsychiatric disorders such as schizophrenia (Chen *et al.*, 2021).

Vascular cognitive impairment (VCI) refers to severe difficulties in the pathological process of learning and memory accompanied by aphasia, agnosia, and disuse, caused by abnormal brain senior intelligence processing related to learning, memory, thinking, and judgment (Meng *et al.*, 2020). VCI has three clinical subtypes, namely, mixed dementia,

vascular dementia (VaD), and mild cognitive impairment (MCI). Bowler and Hachinski (1995) proposed that VCI is the only cognitive impairment type that can be prevented and controlled during the mild stage.

With neuroimaging, VCI (often in a relationship by apparent AD pathology) may well continue even without the rise of new cerebral infarcts, and white matter abnormalities (Smith, 2017). It led to the growing acknowledgement of the role of small vessel disease (including lacunes and leukoaraiosis). Currently, CSVD is recognized as a key mechanism of VCI with a correlation to neurodegeneration. Improvements in MRI have permitted a better picture of the effects of CSVD (Wardlaw *et al.*, 2013).

Table 2.2: Several cerebral small vessel disease (CSVD) manifestations according to STRIVE (Wardlaw *et al.*, 2013).

CSVD manifestation	**Description**
Recent small subcortical infarcts	fresh, small (less than 20 mm in axial section) ischemic lesions concerning perforating arteries, whose radiological features or clinical signs and symptoms indicate their formation in the few weeks before the test; best seen in the DWI sequence; these changes are hypointense in the T1 sequence, hyperintense in the T2 and FLAIR sequences, and isointense in the GRE-T2 sequence
Lacunae of presumed vascular origin	round or oval subcortical lesions 3−15 mm in diameter, filled with fluid, with the cerebrospinal fluid-like signal; these lacunae correspond to a history of acute cerebral infarction or bleeding from the area of vascularization of the perforating artery; the lesions are characterized by a distinctive image in the FLAIR examination; each lesion is a cavity filled with cerebrospinal fluid and surrounded by a hyperintense rim; they are isointense in the DWI sequence, hypointense in the FLAIR and T1 sequences, and hyperintense in the T2 sequence
White matter hyperintensities	symmetric regardless of size; hyperintense in the T2, FLAIR and GRE-T2 (gradient-echo T2) sequences; isointense in DWI; and hypointense in T1
Enlarged perivascular spaces (Virchow–Robin spaces)	mostly seen in basal ganglia <2 mm in size; they usually accompany hyperintense lesions of the white matter and lacunar condition but not brain atrophy; the lesions are hyperintense in T2 sequences, hypointense in FLAIR and T1 sequences, and isointense in the GRE-T2 sequence
Cerebral microbleeds (CMBs)	small, homogeneous lesions <10 mm in diameter, characterized by the 'blooming effect'; the lesions are best seen in the gradient-echo T2 sequence (hypointense lesions); in the T2, T1 and FLAIR sequences, they are isointense; microbleeds correspond to hemosiderin-loaded macrophages that are present in the perivascular space
Brain atrophy	brain atrophy in the context of CSVD is considered only when the patient has not suffered a stroke or head injur

DWI – diffuse-weighted imaging; FLAIR – fluid-attenuated inversion recovery.

2.4 Neuroimaging Modalities in Understanding of Heterogenous CSVD

In brief, several diagnostic modalities are routinely used in clinical practice. To date, neuroimaging is the gold standard to access CSVD, which can visualize and analyse cerebral cortical white matter for a better understanding of disease progression (Gurol *et al.*, 2020; Kaiser *et al.*, 2014). Table 2.3, summarize the diagnostic modalities advantages and disadvantages and their correlation to CSVD.

However, from the table, MRI is most widely used as a neuroimaging technique in CSVD. It is the most common procedure after CT, employed by hospitals worldwide and the most sensitive tool to access CSVD. MRI had transformed into tools advancing research into functional and structural alterations in the healthy and disease brain by providing details of non-invasive images (i.e., brain It also distinguishes soft tissue better than CT and is better at differentiating fat, water, muscle, and other soft tissue.

Table 2.3: Comparisons of different types of diagnostic modalities in the detection of CSVD – their advantages and disadvantages.

Neuroimaging	Advantages	CSVD correlates	Disadvantages	Reference
PET	Non- invasive Give a better understanding of anatomy-pathomechanism of neurological disease. Able to support the clinical diagnosis by visualizing cerebral functions in affected brain regions. Able to differentiate the vascular and degenerative cognitive impairment.	Reduce cerebral blood flow, elevate oxygen extraction fraction, normal oxygen metabolic rate and preserve ^{11}C-flumazenil binding in ischemic brain	Used radioactive components. Quite expensive and limited availability	(Evans *et al.*, 2017; Heiss, 2018; Kitagawa *et al.*, 2009)
CT	Able to detect morphologic lesions. Widely available, easy fast and cost-effective. Enable more full-bodied diagnosis of stroke subtypes.	Hypodensity in basal ganglia in cases of deep cerebral infarction	Lack of sensitivity to diagnose acute ischemia in the brain. Exposure to radiation PCT and/or CTA are invasive and result frequently misinterpreted with limited visualization of distal occlusion.	(Brazzelli *et al.*, 2009; Khan *et al.*, 2007; Pantoni *et al.*, 2014)

Notes: PET- Positron Emission Tomography; CT- Computed Tomography

Table 2.3: Continued.

Neuroimaging	Advantages	CSVD correlates	Disadvantages	Reference
Conventional MRI (cMRI)	Non-invasive, easy, and fast Widely used for detection and quantification of cerebral micro-architectural damage Enable detection of earlier stages of CSVD and more direct biomarkers of the underlying pathophysiology and lacunar infarcts, white matter lesion (WML), and CMB. High in sensitivity and specificity for detecting pathologic changes	Medial lemniscus hyperintensities seen on MRI-FLAIR images are reliable radiologic markers of advanced CVSD. Small lacunas in the ageing brain or bright areas of small non-cavitated high signal intensity on FLAIR, T2-weighted MRI as an indicator for CSVD	Required technical expert for handling and maintenance. Restricted to only visualized 2D white matter damage and unable to provide information regarding the tract involved in related disease. Abnormalities in single penetrating arteries cannot yet be consistently and reliably visualized for use in daily clinical practice	(Jones and Cercignani, 2010; Valdés Hernández *et al.*, 2015)
MRI-DWI	Do not require a contrast medium Fast technique Provides qualitative and quantitative information	Most sensitive sequence for acute ischemic lesions detection within the first few hours after onset. Increased ADC values with WMHs	Limitation in the representation of anisotropic diffusion in neuronal tissues. Relatively poor spatial resolution Lack of specificity Lack of standardized image acquisition protocols and data analysis procedures that restrict the application of DWI and reproducibility of apparent diffusion coefficient values.	(Drake-Pérez *et al.*, 2018; Lin and Chen, 2015)

Notes: MRI – Magnetic Resonance Imaging; DWI – Diffusion-Weighted Imaging

Table 2.3: Continued.

Neuroimaging	Advantages	CSVD correlates	Disadvantages	Reference
MRI-DTI	Non-invasive Give powerful insight about WMI and damage. Plausible indicator of CSVD severity and better informs about age-related white matter deficits and related CSVD. Tractography enabled to tract down and visualize the white matter microstructures in vivo.	Decreased FA in the region of white matter infarcts including SBI. Increased FA is in the region of hypo-perfused WM which depicts some ischemic microstructural changes. Age-related reduced in FA in frontal white matter, the posterior limb of the internal capsule (PLIC) and the genu of corpus callosum (CC)	Laborious pipeline processing Insensitivity of tensor estimation in voxels characterised by low FA values. Inability to resolve intra-voxel fibre orientations	(Farquharson *et al.*, 2013; Lope-Piedrafita, 2018; Nitkunan *et al.*, 2006; Van Hecke and Emsell, 2016)
fMRI	Potential biomarker indicating the health of cerebral microvasculature and CSVD progression. Exact cerebral location (cortical and subcortical) with certain neuronal activities can be commonly studied especially the extent of neuronal activities in cerebrovascular disease	CSVD related white matter hyperintensities and ageing, there is a significant decrement in T2* weighted BOLD signal contrast	Expensive Time-consuming Still evolving and improving	(Amaro Jr and Barker, 2006; Figley *et al.*, 2015; Mascalchi *et al.*, 2014; Matthews *et al.*, 2006)
MRA	Excellent and commonly used for visualization of cerebral vessel occlusion and disease	MRA abnormalities were considered significant if stenosis was more than 50%	Invasive (used of contrast agent)	(Degnan *et al.*, 2012)

Notes: DTI – Diffusion Tensor Imaging; fMRI – Functional Magnetic Resonance Imaging; MRA – Magnetic Resonance Angiography.

2.4.1 Magnetic Resonance Imaging (MRI)

MRI is an imaging procedure that offers in vivo classification of any noticeable cerebral alterations using a very powerful magnetic field that is a thousand-fold stronger than earth's natural magnetic field. The principle of MRI revolves around utilizing the powerful magnetic field (quantified in the Tesla unit varying from 0.05T to 9T) to hydrogen nuclei of water molecules to attract the body of atomic nuclei. This offers obtaining information such as brain tissue volume and WMHs (Heye *et al.*, 2015).

2.4.2 Basic principle of MRI

MRI scan works as an imaging technique because of the distinctive makeup of the human body by producing detailed images under a strong magnetic field. Magnetic field measure in Tesla unit and Conventional MRI (cMRI) scanner produces 1.5 T, powerful enough to pull typical sized car toward its magnetic core. The human body is made up of almost 70% water from all kinds of natural components include minerals, protein, as well as fat (B. Heymsfield *et al.*, 1997). Under normal conditions, water molecules float around freely in nearly all parts of the body. The anatomic composition of water is two hydrogen atoms and one oxygen atom (H_2O) with important hydrogen nuclei and protons.

A magnet embedded inside an MRI scanner can act on a free charged cation (H^+) and trigger the cation to 'spin' in an equal manner or align with the path of the force field. By applying radiofrequency (RF) pulse and differing the intensity and path of the force field, the direction of 'spin' of the proton can be manipulated that enables the build-up of scanning details. Once the RF pulse is turned off, the proton slowly returns to its previous state. This method is called relaxation. Distinct tissue types inside the body revert at distinct speeds then it allows visualization and differentiation between different tissue of the body. The higher the